Landslides (2012) 9:189–203
DOI 10.1007/s10346-011-0284-6
Received: 7 October 2010
Accepted: 12 July 2011
Published online: 31 July 2011
© Springer-Verlag 2011

Jérôme Lopez Saez · Christophe Corona · Markus Stoffel · Laurent Astrade · Frédéric Berger · Jean-Philippe Malet

Dendrogeomorphic reconstruction of past landslide reactivation with seasonal precision: the Bois Noir landslide, southeast French Alps

Abstract The purpose of this study was to reconstruct spatiotemporal patterns of past landslide reactivation in a forested area of the Barcelonnette Basin (Bois Noir landslide, Southern French Alps). Analysis of past events was based on tree ring series from 79 heavily affected Mountain pine (*Pinus uncinata* Mill. ex Mirb) trees growing near or next to the landslide body. Dendrogeomorphic analysis focused on the presence of compression wood and growth reductions, with the first reaction being used for a dating of past reactivations with seasonal precision. A total of 151 growth disturbances were identified in the samples representing eight different stages of reactivation of the landslide body between 1874 and 2008. The spatiotemporal accuracy of the reconstruction is confirmed by historical records from neighboring sites and by aerial photographs. The onset of compression wood formation allows identifying five stages of landslide reactivation during the dormant season or the very beginning of the growing season of trees, i.e., between early October and late May, and three stages toward the end of the growth period. Monthly rainfall data from the HISTALP database demonstrate that the rainfall during four out of the eight reactivations are characterized by summer rainfall totals (July–August) exceeding 200mm, pointing to the important role of summer rainstorms in the triggering of events at the Bois Noir landslide body.

Keywords Dendrogeomorpholoy · Landslides · Growth disturbances · Seasonal precision · French Alps

Introduction

Landslides constitute a common mass movement process and a widespread hazard in mountain and hillslope environments (Shroder et al. 2012) where they repeatedly cause damage and destruction to settlements, transportation corridors, or even lead to the loss of life. To avoid damage or fatalities, data are needed on the frequency and magnitude of past events to perform an appropriate hazard assessment (Jakob and Bovis 1996). Such knowledge is also crucial for the understanding of the variability of landslide processes during historical times and for the establishment of relationships between landslide occurrences and their triggers. The easiest way to model the response of landslide activity to precipitation, for instance, is to plot historical precipitation time series against the temporal pattern of landslide activity and to identify a precipitation threshold which effectively discriminates periods with from periods without landslides (Buma 2000).

A major obstacle for such an analysis is the lack of data with satisfying spatial resolution or precision over medium to long timescales and on a continuous basis (Claessens et al. 2006; Thiery et al. 2007). Usually, the temporal distribution of landslide events is estimated at supradecadal timescales and derived from large inventories of historical archives such as narrations, paintings, engravings and other artworks, terrestrial or aerial photographs, satellite images, or incidental statements (Brunsden and Jones 1976; Hovius et al. 1997; Martin et al. 2002). However, difficulties are normally numerous in accessing, extracting, organizing, databasing, and analyzing such data because they have not usually been collated for scientific purposes. Problems may involve conscientiousness of the observer, editing and recording process issues, and the haphazard nature of recorded events in both time and space (Ibsen and Brunsden 1996). Furthermore, archival data are always biased toward catastrophic events (Flageollet et al. 1999) and are undersampled in unpopulated areas (Mayer et al. 2010). Additional bias is introduced when interviewing residents because human memory is short-lived and highly selective, and the record will contain more frequent events of the recent past (Mayer et al. 2010).

Therefore, archival records should be supplemented with other techniques (Ibsen and Brunsden 1996; Jakob 2005). An accurate method for the reconstruction of events on forested landslides is dendrogeomorphology, i.e., the analysis of trees affected by past geomorphic activity (Alestalo 1971; Stoffel and Bollschweiler 2008). Although a catastrophic failure will destroy all trees on a landslide, trees on shallow landslides characterized by small displacement amplitudes and low velocities may survive to reactivation events and conserve externally visible evidence of past events such as topped, tilted, or S-shaped stems, scars on the stem surface, or root breakages (Carrara and O'Neill 2003; Stefanini 2004). The impacts of such external damage is recorded in the tree ring record, and dendrogeomorphic techniques have successfully been applied in the past to reconstruct landslide histories on sites lacking long and complete archival records.

In contrast to rockfall (Stoffel et al. 2005a, b) or debris flows (Stoffel et al. 2008; Bollschweiler et al. 2010) where scars and tangential rows of traumatic resin ducts have been used to assess past process activity with up to monthly resolution (Bollschweiler et al. 2008; Stoffel and Hitz 2008; Schneuwly et al. 2009), dendrogeomorphology has only rarely been used to assess the seasonality of shallow landslides so far.

Therefore, the aim of this study was to reconstruct spatiotemporal patterns of landslide reactivation at Bois Noir (Barcelonnette Basin, Alpes de Haute-Provence, France). Through the analysis of tree ring series of Mountain pine (*Pinus uncinata* Mill. ex Mirb) we (1) reconstruct landslide activity and years of reactivation, (2) determine the spatial extent of the landslide complex, (3) assess the seasonality of landslide reactivation for the past 130 years, and (4) establish relationships between landslide reactivation and climate characteristics by comparing the landslide chronology with rainfall records.

Study site

The Bois Noir landslide (44°23′27 N, 6°45′27 E; Fig. 1a) is located on the south-facing slope of the Barcelonnette Basin, 2.5 km to the

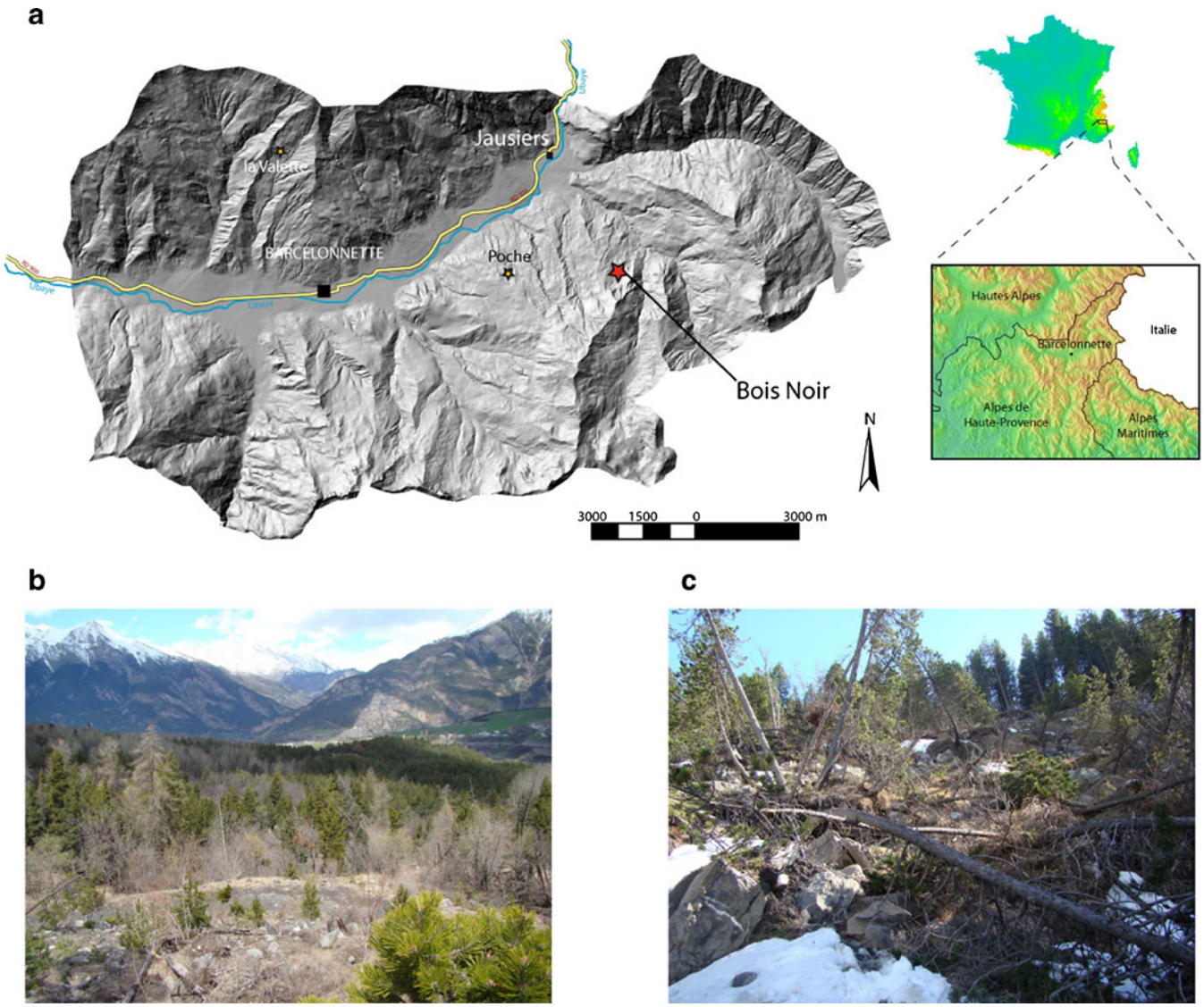

Fig. 1 **a** The Bois Noir landslide is located in the southern French Alps near the village of Jausiers. View of disturbed trees on the scarp (**b**) and in the landslide body (**d**)

southeast of Jausiers (Alpes de Haute-Provence, France). The landslide body is 300 m long, 500 m wide, and ranges from 1,600 to 1,680 m a.s.l. in elevation. The Bois Noir slope segment is characterized by an irregular topography with slope gradients ranging between 10° and 35° (Thiery 2007), and the site is covered by *P. uncinata* and grasslands (Razak et al. 2011). Geology at the study site is characterized by a 15-m-thick top layer of morainic colluvium, underlain by autochthonous Callovo–Oxfordian black marls (BRGM 1974; Flageollet et al. 1999; Maquaire et al. 2003) which are very sensitive to weathering and erosion (Antoine et al. 1995). The southern part of the Bois Noir slope segment is characterized by outcrops of limestone in the summit crest and is characterized by steep slopes of up to 70°, with extensive scree slopes. The area is characterized by a dry and mountainous Mediterranean climate with strong inter-annual rainfall variability. According to the HISTALP meteorological dataset (Efthymiadis et al. 2006), rainfall at the gridded point closest to the Bois Noir landslide (44°25′ N, 6°45′ E) is 1,015±179 mm year^{-1} for the period 1800–2004. Rainfall can be violent, with intensities overpassing 50 mm h^{-1}, especially during summer storms (Flageollet et al. 1999). Mean annual temperature is 7.5°C with 130 days of freezing per year (Maquaire et al. 2003).

These predisposing geomorphic and climatic factors explain the occurrence of a large landslide complex characterized by different styles of activity with shallow rotational and translational shallow slides in the upper parts of the slope, and shallow earthflows in the lower parts of the slope. The landslide complex usually affects the uppermost 2–6 m of the surface deposits. A detailed geomorphologic map (Fig. 2) has been prepared by Razak et al. (2011) from the analysis of a very dense airborne LiDAR point cloud and an associated very high-resolution DTM of 0.25 m using advanced visualization techniques, the interpretation of multi-temporal aerial images, and field observations in 2009. The geomorphologic map combines information on the landslide types, the affected surface deposits, and the relative age of specific features (cracks, lobes) within the landslide complex.

A dense network of small cracks mostly developed with a radial pattern can be observed in the source area upslope of the active

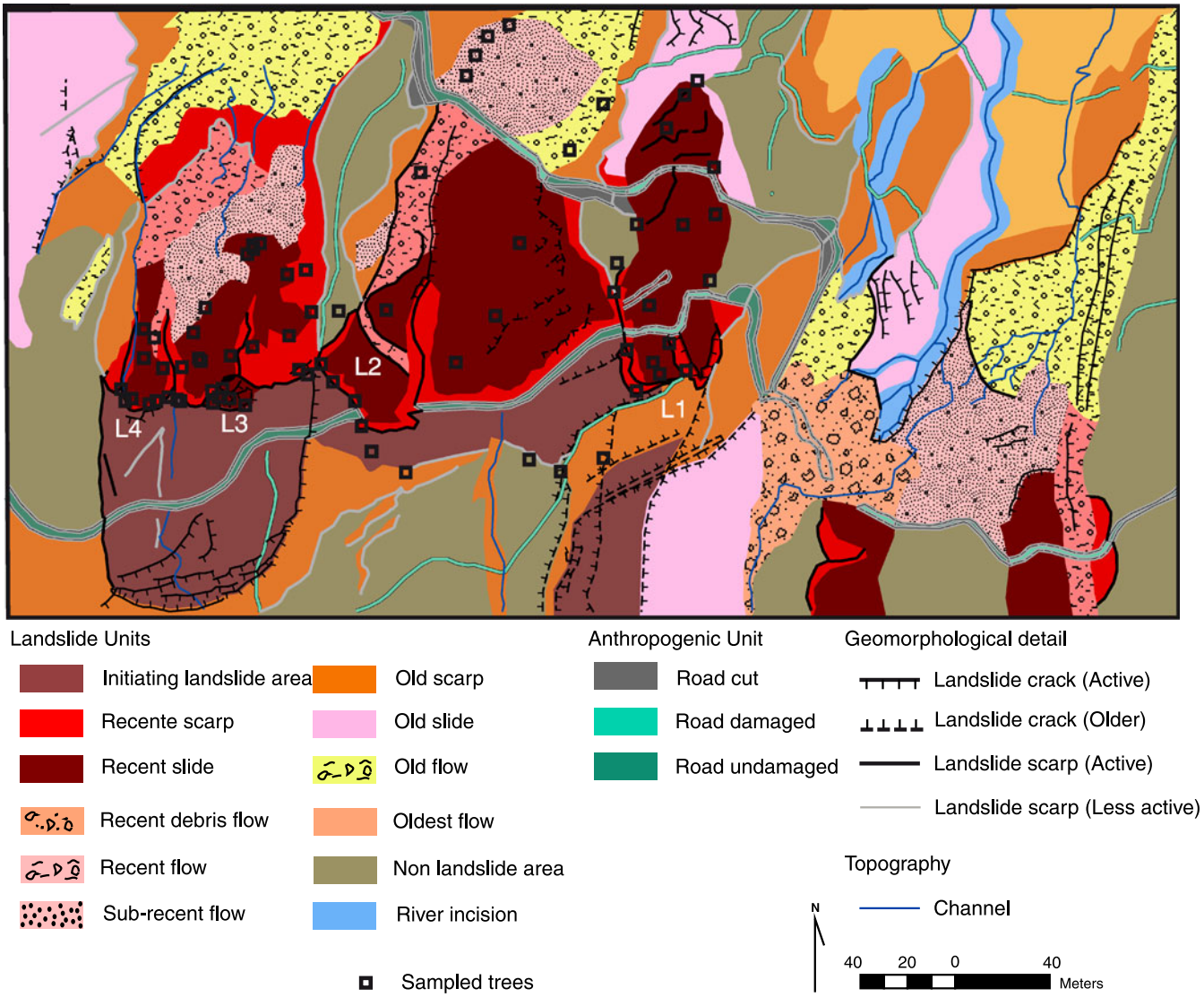

Fig. 2 Geomorphic map (adapted from Razak et al. 2011) and position of trees sampled

landslide complex (Fig. 2). Downhill, the active landslide complex can be subdivided in landslide types of different styles of activity. The upper parts of the source area are characterized by rotational landslide scarps; in the lower parts of the slope, the landslide rigid bodies turn progressively into flow-type bodies characterized by lobes with concentric ridges. Further down, earthflows that reach less steep slopes and that cannot extend laterally are observed and produce pressure ridges.

All the landslide complex has to be interpreted as part of a larger and older landslide affecting more than four times the area of the studied landslide (Razak et al. 2011), and which is characterized by several stages of reactivation.

Landslides represent a major hazard in the Barcelonnette Basin where the combination of predisposing factors (lithology, surface deposits, climate, and land use) create favorable conditions for the triggering of mass movements. Archives yield information on more than 150 landslides in the Barcelonnette Basin since AD 1850 (Amiot and Nexon 1995; Flageollet et al. 1999; Remaître et al. 2010), but only information on one event at Bois Noir, namely in April 1993 (Thiery et al. 2007), is included. This lack of references is partly due to the fact that (1) the Bois Noir landslide complex is not of major interest for risk managers as it does not cause extensive damage to life or property; (2) the Barcelonnette Basin has a relatively low population density, resulting in many slope failures remaining unnoticed; and (3) attention will focus on the extremely active large landslides causing a high potential risk such as La Valette, Super-Sauze, and Poche (Fig. 1a). However, the presence of tilted and deformed trees, of recent scarps and open cracks, and damages to the forest road crossing the slope clearly indicate that there is scope and reason to believe that the Bois Noir landslide has been subjected to multiple stages of reactivation in the recent past (Fig. 1b, c).

Material and methods

Reconstructing landslides events with tree ring series

Dendrogeomorphic techniques have been used to date landslide events in several ways. Tree ages may supply a first but important information on past activity as the oldest undisturbed tree on a

landslide body will provide a minimum age of movement (Carrara and O'Neill 2003). The approach using tree age on landslide surfaces is not new and goes indeed back to the late nineteenth century when McGee (1893) and Fuller (1912) dated movements in Tennessee and along the Mississippi river.

A more detailed analysis of landslide movement involves the interpretation of growth disturbances in annual ring series in trees affected by landslide activity (Carrara and O'Neill 2003). The earliest dendrogeomorphic studies of landslides date back to the 1970s (Alestalo 1971), and the method has been used extensively in the USA (e.g., Reeder 1979; Jensen 1983; Hupp et al. 1987; Osterkamp et al. 1986; Williams et al. 1992; Carrara and O'Neill 2003; Wieczorek et al. 2006), in Quebec (Bégin and Filion 1988). In Europe, tree ring analyses have been used to reconstruct the frequency and extent of landslides events in the French Alps (Braam et al. 1987; Astrade et al. 1998), in the Italian Dolomites (Fantucci and McCord 1996; Fantucci and Sorriso-Valvo 1999; Santilli and Pelfini 2002; Stefanini 2004), in the Spanish Pyrenees (Corominas and Moya 1999), and, more recently, in the Flemish Ardennes (Belgium; Van Den Eeckhaut et al. 2009)

Collection and preparation of samples

The Bois Noir landslide complex has been subdivided into four subunits (called L1, L2, L3, and L4; Fig. 2) according to the geomorphological map and interpretation of Razak et al. (2011). To avoid misinterpretation, trees growing in sectors influenced by other types of geomorphologic processes (e.g., debris flow, gully erosion) or anthropogenic activity (sylviculture) were disregarded for this analysis.

Based on an outer inspection of the stem, *P. uncinata* trees influenced by past landslide activity were sampled in the four subunits. Four cores per tree were extracted: two in the supposed direction of landslide movement (i.e., upslope and downslope cores) and two perpendicular to the slope. To gather the greatest amount of data on past events, trees were sampled within the tilted segment of the stems. We also collected cross-sections from landslide-damaged trees with poor survival probability. In total, 79 *P. uncinata* trees were sampled with four cross-sections and 300 increment cores. For each tree, additional data were collected, such as (1) tree height; (2) diameter at breast height; (3) visible defects in tree morphology, and particularly the number of knees; (4) position of the extracted sample on the stem; (5) photographs of the entire tree; and (6) data on neighboring trees. The coordinate of the tree were obtained with an accuracy <1 m with a Trimble GeoExplorer GPS.

In addition, 20 undisturbed trees located above the landslide scarps and showing no signs of landslide activity or other geomorphic processes were sampled to establish a reference chronology. Two cores per trees were extracted, parallel to the slope direction and systematically at breast height. This reference chronology represents common growth variations in the area (Cook and Kairiukstis 1990) and enables precise cross-dating and age correction of the cores sampled on the landslide body.

The samples obtained in the field were analyzed and the data processed following standard dendrochronological procedures (Braker 2002; Stoffel and Bollschweiler 2009). Single steps of surface analysis included sample mounting on a slotted mount, sample drying, and surface preparation by finely sanding the upper core surface up to grit size 600. In the laboratory, tree rings were counted and ring widths measured to the nearest 0.01 mm using a digital LINTAB positioning table connected to a Leica stereomicroscope and TSAP-Win Scientific software (Rinntech 2009). The reference chronology was developed based on the growth curves of the undisturbed trees using the ARSTAN software (Cook 1985). The two measurements of each reference tree were averaged, indexed, and detrended using a double detrending procedure (Holmes 1994) with a negative exponential curve (or linear regression) and a cubic smoothing spline function (Cook and Kairiukstis 1990). The quality of the cross-dating was evaluated using COFECHA (Holmes 1983) as well as the graphical functions of TSAP-Win (Rinntech 2009). Growth curves of the samples of disturbed trees were then compared with the reference chronology to detect missing, wedging, or false rings and to identify reactions to mechanical stress. As no significant correlation was found between the reference chronology and 16 cores from affected trees (5.3%), these cores were not considered for further analysis.

Sign of disturbance in the tree ring records

Landslide movement (Fig. 3a) may induce several types of growth disturbances (GD) to trees, most commonly in the form of an abrupt reduction in annual ring width (Fig. 3b) and/or the formation of compression wood (CW, Fig. 3c) on the tilted side of the stem.

A reduction in annual ring width over several years (Figs. 3b and 4a) is interpreted as damage to the root system, loss of a major limb, or a partial burying of the trunk resulting from landslide activity (Carrara and O'Neill 2003). In this study, growth ring series had to exhibit (1) a marked reduction in annual ring width for at least five consecutive years such that the (2) width of the first narrow ring was 50% or less of the width of the annual ring of the previous year.

The onset of CW is interpreted as a response to stem tilting induced by pressure on the tree from the landslide material. Tilted trees try to recover straight geotropic growth (Mattheck 1993) via the development of S-shaped morphologies along the trunk. At the level of tree rings, tilting of a conifer trunk will result in asymmetric tree ring growth, i.e., in the formation of wide annual rings with smaller, reddish yellow-colored cells with thicker cell walls (so-called CW; Timell 1986) on the tilted side and narrow (or even discontinuous) annual rings on the opposite side of the tree (Panshin and de Zeeuw 1970; Carrara and O'Neill 2003). For example, the tree illustrated in Fig. 3c was tilted in 1993. The formation of CW on the tilted side of the tree is synchronous with the reduction of ring width in the opposite part of the section.

In the laboratory, wood anatomical analysis and microscopic observation focused on CW formation. Based on data from neighboring sites (Petitcolas and Rolland 1996), we know that the vegetation period of *P. uncinata* locally starts at the end of May with the formation of thin-walled earlywood tracheids. The transition from late earlywood (LE) to latewood (L) occurs in mid-July and the formation of thick-walled latewood tracheids ends in early October. The period between October and May is called the dormancy (D), and there is no cytogenesis during this time of the year (for details and illustrations, see Stoffel et al. 2005a and references therein).

The intra-annual position of CW was determined as illustrated in Fig. 4c–e. In EE, LE, and L, CW is identified by reddish yellow-colored cells with rounded tracheids. In L, a closer examination of

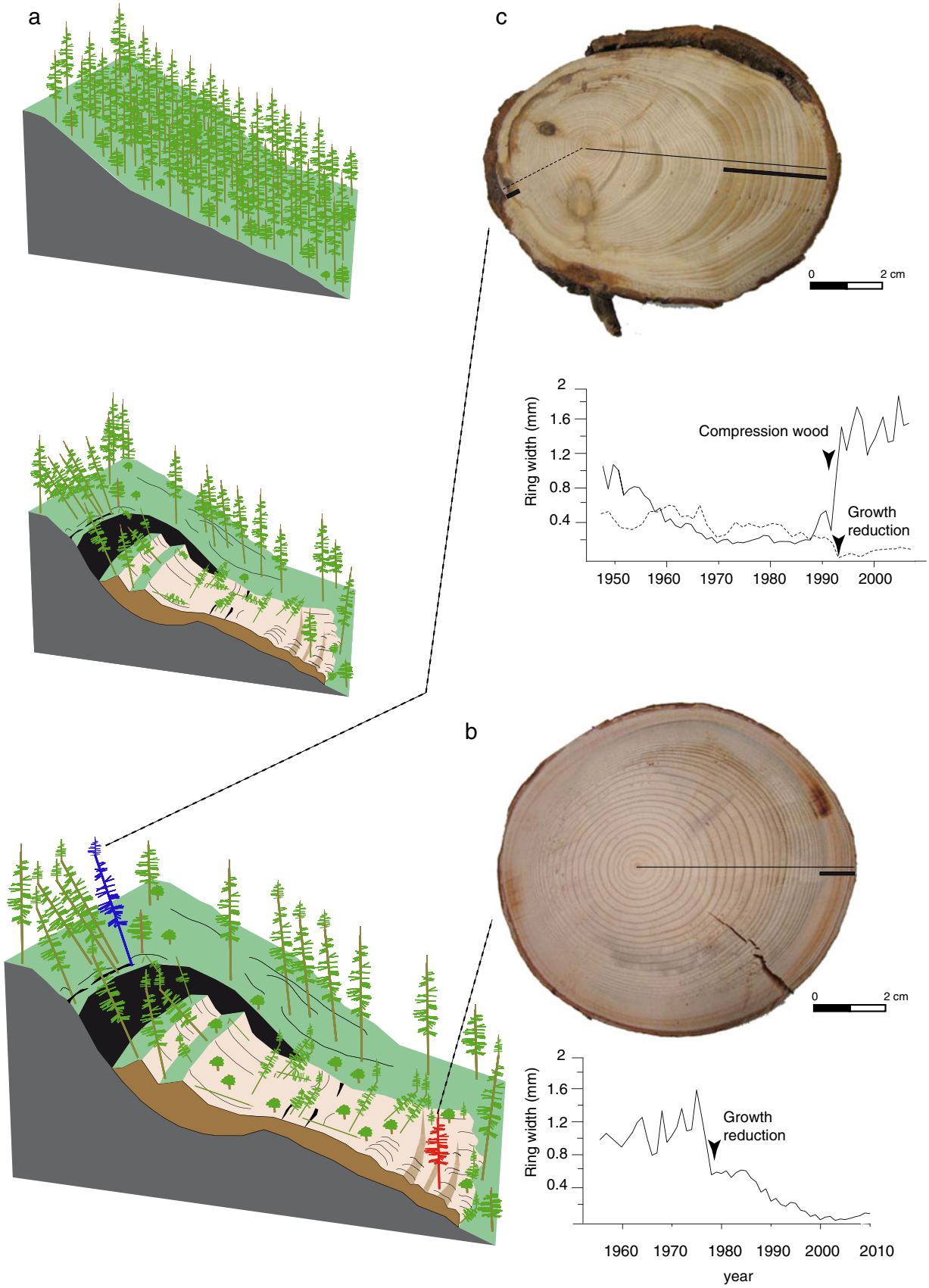

Fig. 3 **a** Principal dendrogeomorphic process event responses resulting from landslide activity. **b**, **c** Evidence used to infer landslide events from growth anomalies in the tree ring record

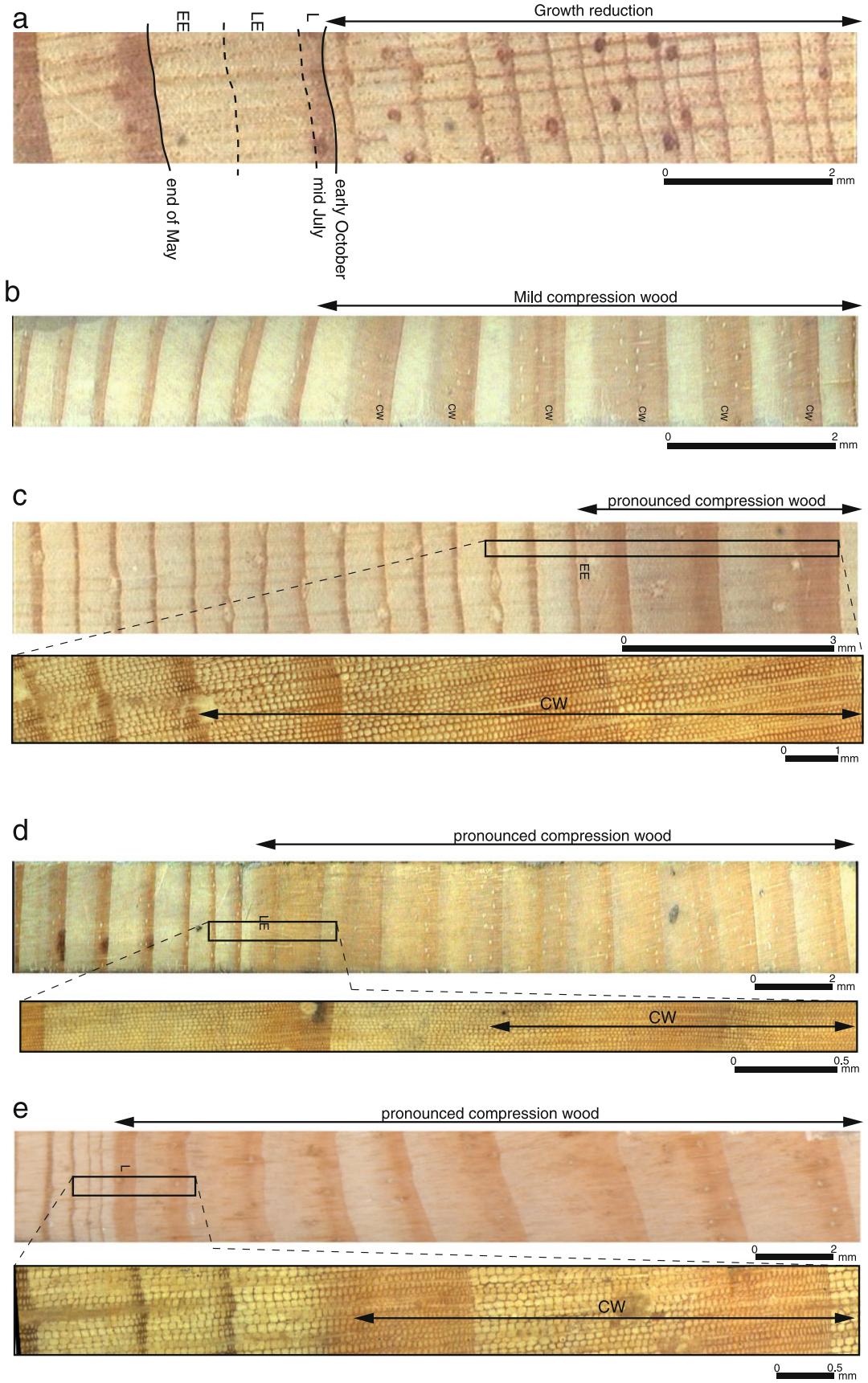
a
EE
LE
L
Growth reduction
end of May
mid July
early October
0
2
mm
b
Mild compression wood
CW
CW
CW
CW
CW
CW
0
2
mm
c
pronounced compression wood
EE
0
3
mm
CW
0
1
mm
d
pronounced compression wood
LE
0
2
mm
CW
0
0.5
mm
e
pronounced compression wood
L
0
2
mm
CW
0
0.5
mm

◀ **Fig. 4** Micro-sections of samples showing an abrupt growth reduction in 1978 (**a**), the onset of a mild CW series restricted to latewood (*L*) in 1947 and the onset of a pronounced CW series (**b**): during the dormant period or in early earlywood (*EE*), between October 2003 and May 2004 (**a**); in late earlywood (*LE*), i.e., between June and mid-July 1947 (**d**); and in latewood (*L*, i.e., between mid-July and early October) 1963 (**e**)

the tracheids of the pronounced CW revealed additional characteristic abundant intercellular spaces. The presence of CW in the first rows of cells (early earlywood, EE) of the first tree ring of a CW series points to tree tilting during the dormant season (Fig. 4c). The onset of CW in any other part of the tree ring (LE, L) does not, in contrast, systematically involve a tilting during the growing season: Pronounced CW is being present in most of or even in the entire width of a tree ring, while weak or moderate CW will only be formed in the later portions of a tree ring (LE, L; Timell 1986). As a result, CW series occurring during the growing season were only taken into account as such if (1) the first appearance of CW was in EL or L and if (2) the signal persisted after the initial occurrence over several tree rings and in their entire width (Fig. 4d, e). In contrast, weak or moderate CW that was, in addition, restricted to EL or L of a CW series, was not used for the assessment of seasonality of tilting (Fig. 4b).

Dating of events

Determination of events was based on the number of samples showing GD in the same year and the distribution of the affected trees on the landslide (Bollschweiler et al. 2008). To avoid overestimation of GD within the tree ring series in more recent years because of the larger sample of trees available for analysis, we used an index value (I_t) as defined by Shroder (1978) and Butler and Malanson (1985):

$$I_t = \left(\sum_{i=1}^{n} (R_t) / \sum_{i=1}^{n} (A_t) \right) \times 100 \qquad (1)$$

where R is the number of trees showing a GD as a response to a landslide event in year t and A is the total number of sampled trees alive in year t. Following disturbance by an initial event, a tree may not necessarily yield useful data on additional events for some time (i.e., a tree may already be forming a narrow band of annual rings such that a subsequent disturbance would not be detected); this is why I was adjusted to only take account of trees with a useful record for year t (Carrara and O'Neill 2003). Following Dubé et al. (2004), Reardon et al. (2008), Butler and Sawyer (2008), and Corona et al. (2010) who reconstructed temporal information on past snow avalanches, the chronology of past events was based on $I \geq 10\%$ of all samples alive at year t. This threshold minimizes the risk that GD caused by other (geomorphic) processes could mistakenly be attributed to a landslide event. We also required that a minimum of five trees exhibits a response in order to avoid an overestimation of response percentage resulting from a low number of trees early in the record (Dubé et al. 2004). A landslide event was thus considered as an event with $I \geq 10\%$ and with GD in at least five trees.

To avoid misclassification of event years due to the strictness of the above thresholds, the position of each tree and its years with GD were included in a Geographical Information System (GIS) using ArcGIS 9.3 (ESRI 2005) as geo-objects, and information from the database were linked as attributes to each single tree.

The age structure of the stand was approximated by counting the number of tree rings of selected trees. However, since trees were not sampled at their stem base and the piths as well as the innermost rings of some trees were rotten, the age structure is biased and does neither reflect inception nor germination dates. Nonetheless, it provides valuable insights into the major disturbance events at the study site with reasonable precision.

Meteorological dataset

The relationship between the actual triggering of landslides and rainfall depends on the characteristics of the movement: Shallow landslides are triggered by heavy rains falling in the hours or days preceding an event, whereas deeper landslides are usually related to the total rainfall recorded over several weeks or months, and deep-seated movements can even be related to the yearly amount of precipitations (e.g., Corominas and Moya 1999; Flageollet et al. 1999; Stefanini 2004). At Bois Noir, the depth of the landslide complex is estimated at 2–6 m (Thiery et al. 2007)

Furthermore, dendrogeomorphology will yield dates of landslide reactivation with seasonal accuracy, but the exact date within a dendrochronological year will remain unknown (Corominas and Moya 1999). For these reasons, this study did not focus on the relationship between landslide occurrences and heavy rainfall over short periods. Mean monthly values are considered to provide an appropriate level of resolution for analyses (Hebertson and Jenkins 2003).

Monthly homogenized precipitation records were taken from the HISTALP dataset (Efthymiadis et al. 2006) consisting of a dense network of 192 meteorological stations extending back to AD 1800 and covering the Greater Alpine Region (4–19° E, 43–49° N, 0–3,500 m a.s.l.). It consists of station data gridded at 0.1×0.1° latitude and longitude, which were 44°25′ N and 6°45′E in the case of this study. The correlation coefficients (not presented) between the HISTALP series and the observed records from the Barcelonnette meteorological station (available for the period 1954–2003) are significant at $p < 0.05$ for all months.

Several classification and regression tree (CART; Breiman et al. 1984; Ripley 1996) analyses were investigated to predict landslide event years from the set of historic climate data (Hebertson and Jenkins 2003) using the 'rpart' routine (Therneau and Atkinson 1997) of the R package (R Development Core Team 2007). CART is a statistical method that explains the variation of a response variable (i.e., landslide indices, I_t, in the present case) using a set of explanatory independent variables, so-called predictors (i.e., monthly climatic data). The method is based on a recursive binary splitting of the data into mutually exclusive subgroups within which objects have similar values for the response variable (see Breiman et al. 1984 for details). Several CART models were tested with monthly, seasonal, and annual combinations of predictors and years from 1874 to 2004 and grouped into two response classes. Years with $I_t < 10\%$ were attributed the class 0, and years with $I_t > 10\%$ the class 1. Predictors were chosen to cover a large time range in order to evaluate a potential delay between rainfall, landslide triggering, tilting, and CW formation (Timell 1986). Monthly precipitations from

previous June to current April (current May to current September) were successively tested as predictors when CW was observed in EE (in any other part of the tree ring, LE, L).

The relation between climatic variables and landslide events was further explored using logistic regression (Aldrich and Nelson 1984; Hebertson and Jenkins 2003). This method describes the relationship between a dichotomous response variable, the presence/absence of a landslide event in our case, and a set of explanatory variables, the climatic data herein. It addresses the same questions as a least squares regression (OLS). In logistic regression, however, one estimates the probability that the outcome variable assumes a certain value rather than estimating the value itself by fitting data to a logistic curve. The logit is simply the log odds ratio of mean landslide probability:

$$\log \mathrm{it}(p_i) = \left(\frac{p_i}{1-p_i}\right) \quad (1)$$

where p is the probability of a major landslide year for the i years (1874–2004 herein).

It is modeled as a linear function:

$$\log \mathrm{it}(p_i) = \beta_o + \beta_1 x_{1,i} + \ldots + \beta_k x_{k,i} \quad (2)$$

With an equivalent formulation:

$$p_i = \frac{1}{1 + e^{-(\beta_o + \beta_1 X_{1,i} + \ldots + \beta_k X_{k,i})}} \quad (3)$$

where X_k represents the k climatic factors used as regressors for year i, β_o the intercept, and β_k the regression coefficients.

The unknown parameters β_j are usually estimated by maximum likelihood using a method common to all generalized linear models.

Results

Age structure of the stand and growth disturbances

The oldest tree cored at Bois Noir shows 173 tree rings at sampling height (AD 1837), while 50 growth rings (AD 1958) where counted in the youngest tree. Trees growing in or around the landslide body have a mean age of 100 years with a standard deviation of 23 years. Figure 5 illustrates the spatial distribution of tree ages. The age pattern of the stand is heterogeneous in L1, but tends to be more homogenous in the upper part of L2, L3 and in the upper eastern part of L4, near the scarp area, where a majority of trees are 100–120 years old. In the upper western part of L4, *P. uncinata* are younger with 60–80 years. The spatial gap in the lower part of L3 and L4 is related to the presence of shrubs and young broadleaved trees which were not sampled in this study.

Summary of disturbance in tree ring record

Analysis of the 79 trees sampled on the landslide allowed identification of 151 GD relating to past landslide events, with the onset of CW (82 GD, 55%) being more common than abrupt growth reductions (69 GD, 45%; Table 1). In 1859, the sample size surpassed the n=10 threshold for landslides to be considered events using dendrogeomorphic methods (Fig. 6). Sample size increased markedly after 1890 and excelled 50% (n=40) in 1912. The earliest GD observed in the tree ring series was dated to AD 1853; however, this year was not considered a landslide event as only two trees showed reactions. In contrast, the relative number of trees with GD did exceed the 10% threshold in 9 years after AD 1859 and were therefore considered years with landslide reactivation (Fig. 6). Apart from the landslide recorded in local archives in 1993, eight additional previously undocumented events took place between 1875 and 2008, namely in 1875, 1897, 1947, 1963, 1977, 1978, 2000, and 2004.

Seasonal timing of CW formation

Analysis of the intra-seasonal position of CW was used to determine the seasonal timing of tilting at Bois Noir landslide.

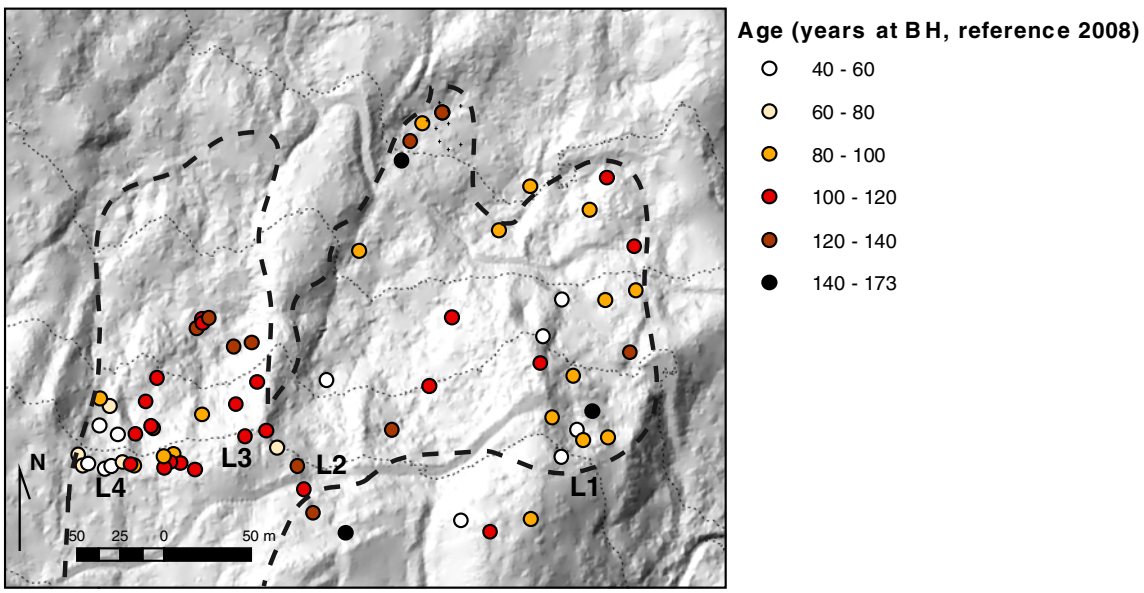

Fig. 5 Mean age of *P. uncinata* Mill ex. Mirb trees sampled on the Bois Noir landslide body

Table 1 Growth disturbances corresponding to past landslide reactivations listed by year and type

Year of GD	GD (*n*)	GR (*n*)	CW (*n*)	EE (%)	LE (%)	L (%)	Season of reactivation
2004	10	5	5	100	0	0	October 2003–April 2004
2000	24	8	16	0	0	100	July–September 2000
1993	36	14	22	72	14	14	October 1992–April 1993
1978	28	20	8	100	0	0	July–September 1977
1977	8	0	8	0	0	100	
1963	10	5	5	0	0	100	July–September 1963
1947	19	11	8	63	37	0	October 1946–April 1947
1897	9	4	5	100	0	0	October 1896–April 1897
1875	7	2	5	100	0	0	October 1874–April 1875
total	151	69	82	63	5	32	

GD growth disturbance, *GR* growth reduction, *CW* compression wood, *EE* early earlywood, *LE* late earlywood, *L* latewood

Table 1 shows a clear concentration of CW formation in EE (63%). Considering the timing of annual tree ring formation at Bois Noir, tilting is likely to have occurred between October of the previous and April of the current year in 1874–1875, 1896–1897, 1946–1947, 1992–1993, and 2003–2004. For those events where CW formation was initiated during the growth period of trees, it appears that CW formation is much more frequent during the period of latewood formation (L=32%). In this case, tilting would have occurred between July and September in 1963 and 2000. GD observed in EE 1978 were merged with GD observed in L in 1977 (Table 1). We considered that a unique reactivation occurred between July and September 1977. The onset of CW in EE in 1978 was regarded as delayed CW formation.

The relationship between dated events and spatial data is represented in the event response maps presented in Fig. 7. These maps reveal that major events occurred between October and April in 1946–1947 and 1992–1993 and between July and September in 1977 and 2000. They were recorded by trees located in all subunits of the landslide body (L1, L2, L3, and L4). Between July and September 1963 and between October 2003 and April 2004, movements affected trees only in the scarp area and on the upper landslide body, in subunits L1 and L4. The position of these tilted trees suggests a propagation of regressive erosion toward the scarp area.

Relationship between landslide occurrences and meteorological data

The best model derived from CART analyses used only July rainfalls to optimize the splitting of landslide events probabilities. The splitting value for July was 153 mm, and the confusion matrix indicates that the model correctly classified non-landslide years in 98% of the cases. The likelihood of correctly classifying landslide events, however, is only 37%: Three out of eight landslide events occurred when precipitation in July was >153 mm. Several logistic regression models were then tested with the presence/absence of a landslide event as a dichotomous response variable and with monthly, seasonal, and annual rainfall as a single predictor. Analysis again confirmed the primordial role of summer precipitations (July, August) in landslide triggering (Table 2 and Fig. 8), and the most parsimonious logistic regression model has been determined having the following general form:

$$\text{Log it}(p_i) = \beta_o + \beta_j(\text{July} + \text{August rainfall})$$

The model provides parameter estimates of −5.62 for β_o and 0.016 for β_j. The chi-square statistics for the model (9.22) are significant with $p<0.05$. The likelihood ratio test, significant at $p<0.05$, indicates that the logit model is better than a null model and the pseudo-R^2 value (0.16) in correctly predicting landslide

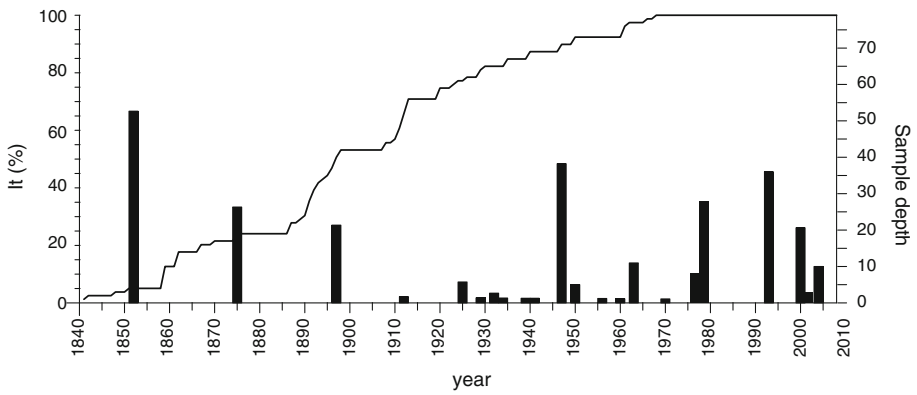

Fig. 6 Event response histograms showing past landslide reactivations and seasonal distribution of the onset of CW formation. The percentage (I_t) of trees responding to an event are given on the *left axis*; the sample depth (i.e., the number of trees available for analysis) is presented on the *right axis*. The *gray line* shows the total number of trees (*n*) alive in each year

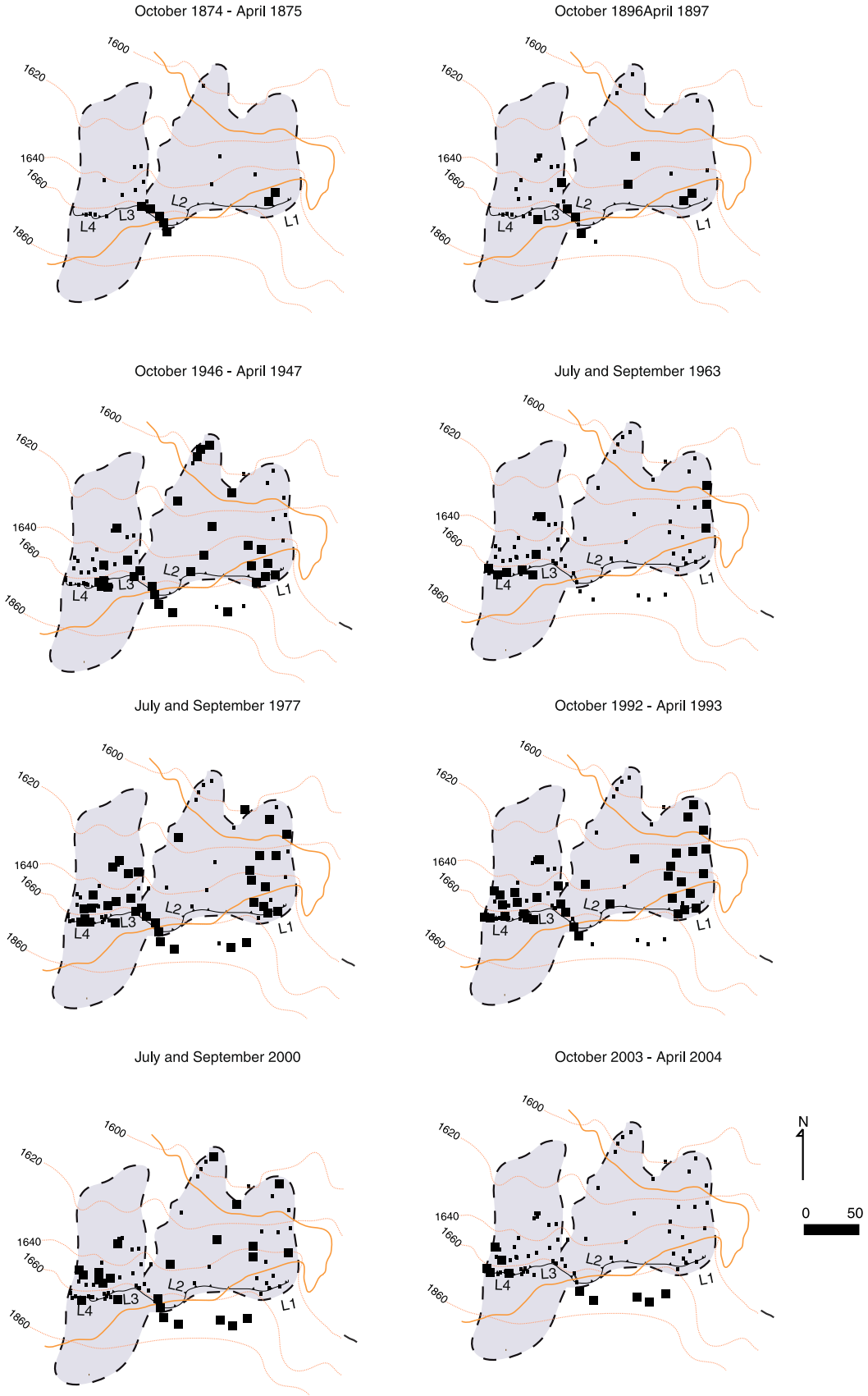

Fig. 7 Event response maps showing the Bois Noir landslide for each of the reconstructed reactivation events. *Large dots* indicate trees disturbed by the mass movement; *small dots* represent trees which are alive but not affected by the reactivation

Table 2 Parameters for logistic regression models of triggering: for each month, the p value, its significance, the intercepts (A) and slopes (B) are given

Month	p value	Significance	A	B
Jul	0.009	<0.01	−4.62	0.021
Aug	0.035	<0.05	−4.11	0.015
Sep	0.35			
Oct	0.07	<0.1	−4.55	0.008
Nov	0.22			
Dec	0.75			
Jan	0.51			
Fev	0.59			
Mar	0.32			
Apr	0.38			
May	0.73			
Jun	0.56			
Jul+Aug	0.004	<0.01	−5.62	0.016

Blank cells are not statistically significant

*$p<0.05$, **$p<0.01$, ***$p<0.1$

triggering probability. The probability of a landslide is 8% for 200 mm July + August rainfall and 15% for 240 mm rainfall (i.e., ninth decile threshold for July + August precipitations; see Fig. 8).

Discussion

Spatiotemporal accuracy of the reconstruction

Dendrogeomorphic analysis of 300 increment cores and four cross-sections taken from 79 *P. uncinata* allowed reconstruction of eight reactivations phases of the Bois Noir landslide between 1874 and 2009. The reconstruction added seven previously unknown events to the local landslide chronology and confirmed the mass movement of 1993 depicted in the literature (Fig. 9). According to the archival records, six of the reactivation years dated for the Bois Noir landslide are characterized by intense landsliding at other sites within the Barcelonnette Basin. Six references on landslides at other nearby sites have been inventoried for 1963, five for 2003–2004, four for 1977 and 1992–1993, three for 1947, and one for 1875 and 2000 (Amiot and Nexon 1995; Flageollet et al. 1999), but this database is incomplete (Remaître et al. 2010). Only the date of 1897 could not be found at other sites of the basin and therefore remains unconfirmed.

The diachronic analysis of aerial photographs between 1948 and 2007 provides additional evidence for the spatiotemporal accuracy of the dendrogeomorphic reconstruction presented in this paper. The existence of the scarp area in 1948 (Fig. 10a) first of all confirms that landslide reactivation predates the first and only historically dated event at Bois Noir of 1993. The reactivation in 1977, deciphered from tree ring records, is supported by the lengthening of the bare area observed on aerial photographs, in

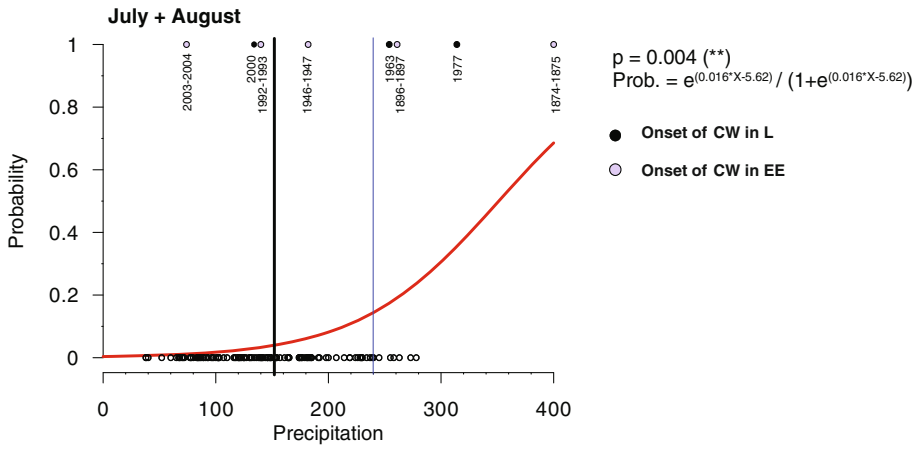

Fig. 8 July + August precipitation values and predicted probabilities of triggering for the Bois Noir landslide. Monthly values for the period 1874–2003 are extracted from the HISTALP database

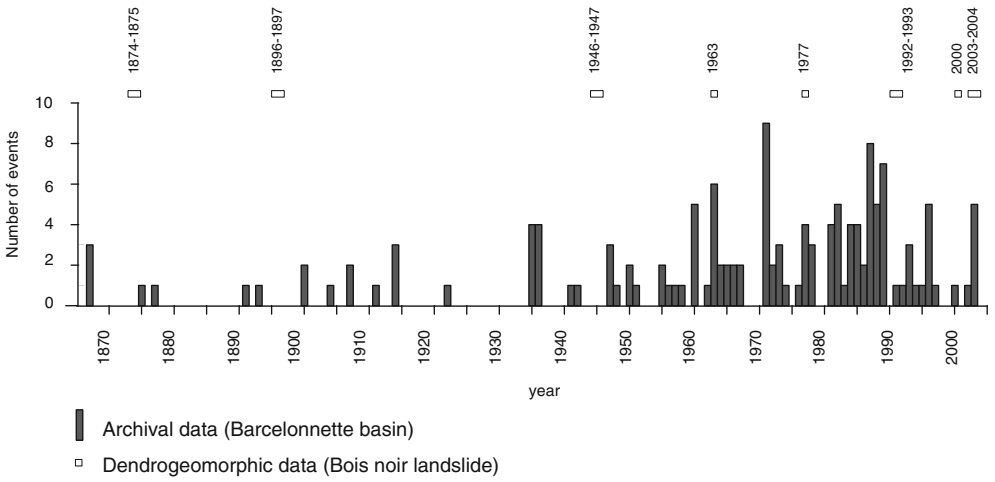

Fig. 9 Number of landslide events (histogram) available from archival data (1869–2006; Flageollet et al. 1999) and reactivations of the Bois Noir landslide obtained with tree ring analysis (*points*)

the four subunits, between 1974 and 1982 (Fig. 10c, d). In addition, significant changes observed at L1 and L4 between 1982 and 2003 (Fig. 10d–f) corroborate the event response maps for the 1993 and 2000 events. In addition, between 1948 and 1974 (Fig. 10a–c) and 2003 and 2007 (Fig. 10f, g), the aerial photographs do not reveal significant changes neither in the landslide body nor in the scarp area, thus supporting the assumption of locally more limited events in 1963 and 2003–2004.

Nonetheless, the reconstructed time series only represent a minimum frequency of reactivation events for the Bois Noir landslide, bust most likely contains a majority of large events for the period considered. In addition, several limitations became apparent as to the potential of tree ring analysis in detecting landslide events. First of all, only reactivations powerful enough to damage (such as topping, tilting, or root damaging), but not killing trees, will remain datable with dendrogeomorphic techniques. Evidences of more destructive events are, in contrast, likely to be lost as dead trees will disappear some time after an event. Second, our reconstruction was limited by the age of the trees established on the landslide body, an element which is partly linked to the frequency of destructive events. Third, it is also obvious that a tree recovering from an initial landslide event and forming very narrow annual rings or CW will be unlikely to develop a signal clearly distinguishable from the first one after a subsequent landslide event (Carrara and O'Neill 2003).

Rainfall conditions for landslide reactivation

Statistical analyses reveal that four out of eight landslide events (1875, 1897, 1963, and 1977) were triggered when July and summer (July–August) precipitations exceeded 153 and 200 mm, respectively. The results suggest that intense summer

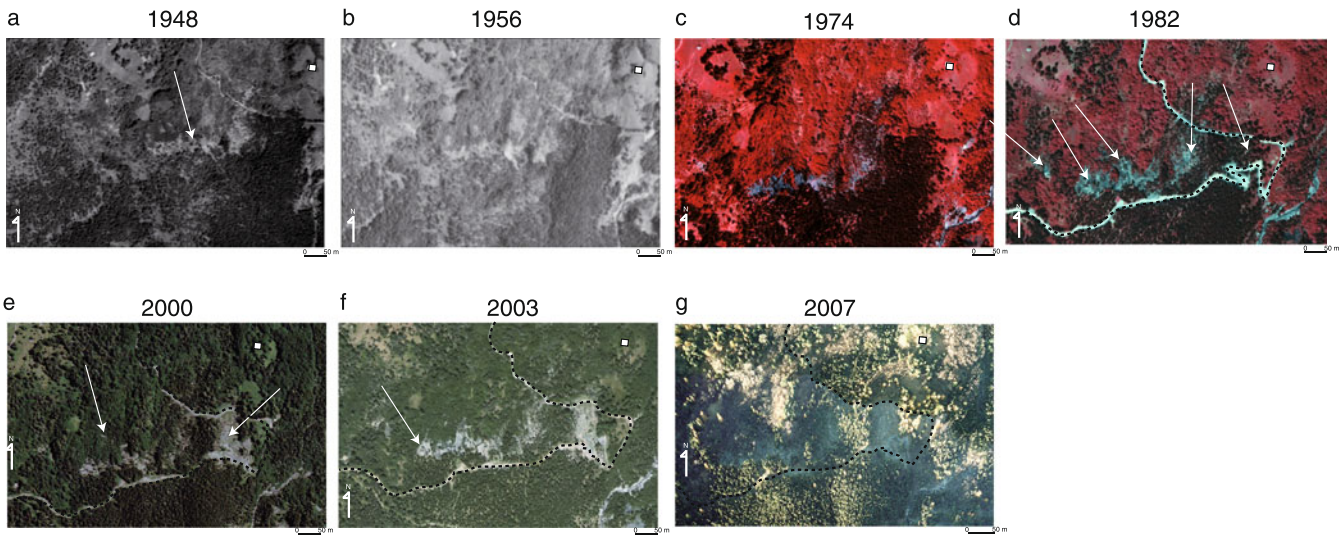

Fig. 10 Diachronic evolution of the Bois Noir landslide between 1948 and 2007. Aerial photographs of the landslide in 1948 (**a**) (National Geographic Institute, aerial mission, 1948_F, 3537-3540_P_30000), 1956 (**b**) (1956_F, 3139-3639_P_25000), 1974 (**c**) (1974_FR_2438_P_17000), 1982 (**d**) (1982_IFN04_P_17000), 2000 (**e**) (2000_FD04_C_250000), 2003 (**f**) (2003_FD06_C_25000), 2007 (**g**) (high-resolution aerial photograph). The *white arrows* indicate landslide movements

rainfalls would play an important role in reactivating landslides at Bois Noir as in the Barcelonnette area: (1) considering the period 1975–2004, the maximum daily rainfall during summer months represents 60% of the monthly totals (Remaître 2006); (2) summer rainstorms can be locally intense, yielding intensities of sometimes more than 50 mm h^{-1} (Flageollet et al. 1999; Remaître et al. 2010). In detail, the onset of CW in LW 1963 and LW 1977 coincide with intense summer precipitations (254 and 314 mm, respectively), therefore suggesting a synchronism between rainfall occurrences and landslide triggering. Conversely, a delay of a few months is observed between intense precipitations in summers 1874 and 1896 (400 and 261 mm, respectively) and the onset of CW in EE 1875 and EE 1897. Two possible explanations exist for this delay: (1) The gradual rise in pore water pressures related to prolonged rainfall events may be the reason for a delayed response to critical triggering conditions (Van Asch and Van Steijn 1991; Matsuura et al. 2008; Razak et al. 2009). (2) On the other hand, it is feasible that the formation of CW was delayed in the present two cases, as shown for other sites by Carrara and O'Neill (2003). However, as the onset of CW formation reveals a synchronous intra-annual response of a majority of tilted trees in 1875 and 1897, we tend to reject this hypothesis.

The rainfall threshold determined in our study therefore seems to confirm findings by Flageollet et al. (1999), stating that 104 out of 134 landslides in the neighboring Vars basin would have occurred in seasons with at least 1 month with >100 mm of rainfall. Nevertheless, these thresholds remain indicative as (1) they were determined with a comparably small number of seasonally dated reactivation events (not statistically significant); (2) the very localized impact of thunderstorms and the scarcity of measuring apparatus in the basin do not enable determination of water amounts effectively falling on site triggering (Flageollet et al. 1999) with any precision; and (3) no unique set of measurements exists to characterize rainfall conditions that are likely to trigger slope failures. Guzzetti et al. (2007), for instance, listed 25 rainfall and climate variables used in the literature for the definition of empirical thresholds for the initiation of landslides. Similarly, in the case of the Bois Noir event recorded in 1993, Flageollet et al. (1999) did not attribute the triggering of the event to the above average precipitations in April but to a combination of distant multi-annual factors with seasonal or monthly parameters. In that case, April rainfalls followed five autumn–winter months which were particularly low on rainfall, but after a year (1992) of excess rainfall following a 10-year period with insufficient rainfall. Other factors such as human action or seismic shocking can directly trigger a landslide. At Bois Noir, a forest road constructed in 1981 may have increased liability to landsliding. This hypothesis is supported by a study focusing on the relationship between land use, human activity, and landslides in Vars (Martin, 1996), where 93% of the events counted between 1820 and 1995 have been linked with some human factor, particularly road laying and widening. Similarly, earthquake triggering of landslides is very common, but not quantitatively understood (Tatard et al. 2011). The Ubaye valley is one of the most active seismic zones in the French Alps (Jenatton et al. 2007) and home of the largest earthquake in the French Alps of the last century (5 April 1959, magnitude, 5.5; Jenatton et al. 2007). In 2003–2004, a prolific and protracted earthquake swarm occurred in the wider study region and reached maximum magnitudes of 2.3 in October 2003. It is therefore possible that the landslide reactivation dated to dormancy 2003–2004 could (also) be the result of shaking.

Conclusion

Dendrogeomorphology has been proven to be a powerful tool in adding substantially to the historic record and spatial assessment of past reactivation of landslide events at Bois Noir. Many reactivations, which remained unnoticed, could be identified and mapped and thus help extend the history of landslides back to the late nineteenth century. Comparison of tree ring data with historical records and aerial photographs clearly demonstrates the spatiotemporal accuracy of the reconstruction. Furthermore, the intra-annual dating of past mass movements through the analysis of the intra-annual position of CW allowed inferring triggers of reactivation. Nevertheless, further investigations are needed, particularly at the regional scale, to take account of the complexity of relations between landslides and climatic conditions.

Acknowledgments

This research has been supported by the DENDROGLISS program, funded by the MAIF foundation and the Cemagref by the PARAMOUNT program, 'ImProved Accessibility, Reliability and security of Alpine transport infrastructure related to MOUNTainous hazards in a changing climate', funded by the Alpine Space Programme, European Territorial Cooperation, 2007–2013. It has also been supported by the EU-FP7 project ACQWA (project no. GOCE-20290). The authors would like to acknowledge J. Corominas and two journal reviewers whose insightful comments helped them improve an earlier version of the paper.

References

Aldrich J, Nelson F (1984) Linear Probability, Logit and Profit Models. Sage Publications, Beverly Hills, CA

Alestalo J (1971) Dendrochronological interpretation of geomorphic processes. Fennia 105:1–139

Amiot A, Nexon C (1995) Inventaire des aléas dans le Bassin de Barcelonnette depuis 1850. Mémoire de Maîtrise de Géographie Physique, Université Louis Pasteur, 173 pp

Antoine P, Giraud D, Meunier M, Van Ash T (1995) Geological and geotechnical properties of the "Terres Noires" in southeastern France: weathering, erosion, solid transport and instability. Eng Geol 40:223–234

Astrade L, Bravard JP, Landon N (1998) Mouvements de masse et dynamique d'un géosystème alpestre: étude dendrogéomorphologique de deux sites de la de la vallée de Boulc (Diois, France). Géographie Physique et Quaternaire 52:153–165

Bégin C, Filion L (1988) Age of landslides along the Grande Riviere de la Baleine estuary, eastern coast of Hudson Bay, Quebec (Canada). Boreas 17:289–299

Bollschweiler M, Stoffel M, Schneuwly DM, Bourqui K (2008) Traumatic resin ducts in *Larix decidua* trees impacted by debris flows. Tree Physiol 28:255–263

Bollschweiler M, Stoffel M, Vázquez-Selem L, Palacios D (2010) Tree-ring reconstruction of past lahar activity at Popocatépetl, Mexico. Holocene 20:265–274

Braam RR, Weiss EEJ, Burrough PA (1987) Spatial and temporal analysis of mass movement using dendrochronology. Catena 6:573–584

Braker O (2002) Measuring and data processing in tree-ring research—a methodological introduction. Dendrochronologia 20:203–216

Breiman L, Freidman JH, Olshen R A, Stone C J (1984) Classification and Regression Trees. Wadsworth

BRGM (1974) Carte et notice géologique de Barcelonnette au 1:50 000ème, XXXV-39. Bureau des Recherches Géologiques et Minières, Orléans
Brunsden D, Jones DKC (1976) The evolution of landslides slopes in Dorset. Philos Trans R Soc Lond Sér A 283:605–631
Buma J (2000) Finding the most suitable slope stability model for the assessment of the impact of climate change on a landslide in southeast France. Earth Surf Processes Landf 25:565–582
Butler D, Malanson G (1985) A reconstruction of snow-avalanche characteristics in Montana, U.S.A., using vegetative indicators. J Glaciol 31:185–187
Butler D, Sawyer CF (2008) Dendrogeomorphology and high-magnitude snow avalanches: a review and case study. Nat Hazards Earth Syst Sci 8:303–309
Carrara PE, O'Neill JM (2003) Tree-ring dated landslide movements and their relationship to seismic events in southwestern Montana. Quat Res 59:25–35
Claessens L, Verburg PH, Schoorl JM, Veldkamp A (2006) Contribution of topographically based landslide hazard modelling to the analysis of the spatial distribution and ecology of kauri (*Agathis australis*). Landsc Ecol 21:63–76
Cook E (1985) A time series analysis approach to tree-ring standardization. PhD thesis, University of Arizona, Tucson
Cook E, Kairiukstis L (1990) Methods of dendrochronology: applications in the environmental sciences. Kluwer, Norwell
Corominas J, Moya J (1999) Reconstructing recent landslide activity in relation to rainfall in the Llobregat river basin, Eastern Pyrenees, Spain. Geomorphology 30:79–93
Corona C, Rovéra G, Lopez Saez J, Stoffel M, Perfettini P (2010) Spatio-temporal reconstruction of snow avalanche activity using tree-rings: Pierres Jean Jeanne avalanche talus, Massif de l'Oisans, France. Catena 83:107–118
Dubé S, Filion L, Hétu B (2004) Tree-ring reconstruction of high-magnitude snow avalanches in the northern Gaspé Peninsula, Québec. Arct Antarct Alp Res 36:555–564
Efthymiadis D, Jones PD, Briffa KR, Auer I, Böhm R, Schöner W, Frei C, Schmidli J (2006) Construction of a 10-min-gridded precipitation data set for the Greater Alpine Region for 1800–2003. J Geophys Res 111:D01105. doi:10.1029/2005JD006120
ESRI (2005) ArcView. http://www.esri.com/software/arcgis/arcview
Fantucci R, McCord A (1996) Reconstruction of landslide dynamic with dendrochronological methods. Dendrochronologia 13:33–48
Fantucci R, Sorriso-Valvo M (1999) Dendrogeomorphological analysis of a slope near lago, Calabria (Italy). Geomorphology 30:165–174
Flageollet JC, Maquaire O, Martin B, Weber D (1999) Landslides and climatic conditions in the Barcelonnette and Vars basins, Southern French Alps, France. Geomorphology 30:65–78
Fréchet J (1978) Sismicité du Sud-Est de la France, et une nouvelle méthode de zonage sismique. Thèse, Univ. Sci. Méd. Grenoble, 159 pp
Fuller ML (1912) The New Madrid earthquake. U.S. Geological Survey Bulletin 494, 119 pp
Guzzetti F, Peruccacci S, Rossi M, Stark CP (2007) Rainfall thresholds for the initiation of landslides in central and southern Europe. Meteorol Atmos Phys 98:239–267. doi:10.1007/s00703-007-0262-7
Hebertson EG, Jenkins MJ (2003) Historic climate factors associated with major avalanche years on the Wasatch Plateau, Utah. Cold Regions Science and Technology 37(3):315–332
Holmes RL (1983) Computer-assisted quality control in tree-ring dating and measurement. Tree-Ring Bulletin 44:69–75
Holmes RL (1994) Dendrochronology program manual. Laboratory of Tree-Ring Research. Tucson, Arizona, USA
Hovius N, Stark CP, Allen PA (1997) Sediment flux from a mountain belt derived by landslide mapping. Geology 25:231–234
Hupp CR, Osterkamp WR,Thornton JL (1987) Dendrogeomorphic evidence and dating of recent debris flows on Mount Shasta, Northern California: U.S. Geological Survey Professional Paper 1396-B, 39 pp
Ibsen ML, Brunsden D (1996) The nature, use and problems of historical archives for the temporal occurrence of landslides, with specific reference to the south coast of Britain, Ventnor, Isle of Wight. Geomorphology 15:241–258
Jakob M, Bovis MJ (1996) Morphometrical and geotechnical controls of debris flow activity, southern Coast Mountains, British Columbia, Canada. Z Geomorphol Suppl 104:13–26
Jakob M (2005) Debris flow hazard analysis. In: Jakob M, Hungr O (eds) Debris flow hazards and related phenomena. Praxis Publishing, Chichester, pp 411–438
Jenatton L, Guiguet R, Thouvenot F, Daix N (2007) The 16,000-event 2003–2004 earthquake swarm in Ubaye (French Alps). J Geophys Res 112:B11304
Jensen JM (1983) The Upper Gros Ventre landslide of Wyoming: a dendrochronology of landslide events and possible mechanics of failure: Geological Society of America Abstracts with Programs, vol 15, no. 5, p 387
Maquaire O, Malet JP, Remaître A, Locat J, Klotz S, Guillon J (2003) Instability conditions of marly hillslopes: towards landsliding or gullying? The case of the Barcelonnette Basin, South East France. Eng Geol 70:109–130
Martin Y, Rood K, Schwab JW, Church M (2002) Sediment transfer by shallow landsliding in the Queen Charlotte Islands, British Columbia. Can J Earth Sci 39:189–205
Matsuura S, Asano S, Okamoto T (2008) Relationship between rain and/or meltwater, pore-water pressure and displacement of a reactivated landslide. Engineering Geology 101(1-2):49–59
Mattheck C (1993) Design in der Natur. Reihe Ökologie 1: Rombach Wissenschaft
Mayer B, Stoffel M, Bollschweiler M, Hübl J, Rudolf-Miklau F (2010) Frequency and spread of debris floods on fans: a dendrogeomorphic case study from a dolomite catchment in the Austrian Alps. Geomorphology 118:199–206
McGee WJ (1893) A fossil earthquake. Geol Soc Am Bull 4:411–414
Osterkamp WR, Hupp CR, Blodgett JC (1986) Magnitude and frequency of debris flows, and areas of hazard on Mount Shasta, California. U.S. Geological Survey Professional Paper 1396-C, 21 pp
Panshin AJ, de Zeeuw C (1970) Textbook of Wood Technology, vol. 1, 3rd ed. McGraw-Hill, New York
Petitcolas V, Rolland C (1996) Dendroecological study of three subalpine conifers in the region of Briançon (French Alps). Dendrochronologia 14:147–153
R Development Core Team (2007) R: a Language and Environment for Statistical Computing. R Foundation for Statistical Computing, Vienna, Austria. http://www.Rproject.org
Razak KA, Straatsma MV, van Westen CJ, Malet JP (2009) Utilization of airborne LiDAR data for landslide mapping in forested terrain: status and challenges. In: Mulyana AK (ed) Proceedings of the 10th South East Asian Survey Congress (SEASC), Bali, Indonesia, 10 pp
Razak KA, Straatsma MW, van Westen CJ, Malet JP, de Jong SM (2011) Airborne laser scanning of forested landslides characterization: terrain model quality and visualization. Geomorphology 126(1–2):186–200. doi:10.1016/j.geomorph.2010.11.003
Reardon BA, Pederson GT, Caruso CJ, Fagre DB (2008) Spatial reconstructions and comparisons of historic snow avalanche frequency and extent using tree rings in Glacier National Park, Montana, U.S.A. Arct Antarct Alp Res 40:148–160
Reeder JW (1979) The dating of landslides in Anchorage, Alaska—a case for earthquake triggered movements. Geological Society of America Abstracts with Programs, vol 11, no. 7, p 501
Remaître A (2006) Morphologie et dynamique des laves torrentielles: application aux torrents des Terres Noires du bassin de Barcelonnette (Alpes du Sud). Thèse de Doctorat, Université de Caen-Basse-Normandie, p 487
Remaître A, Malet JP, Cepeda J (2010) Landslides and debris flows triggered by rainfall: the Barcelonnette Basin case study, South French Alps. In: Malet J-P, Casagli N, Glade T (eds) Proceeding sof the International Conference 'Mountain Risks: Bringing Science to Society', 24–26 November 2010. CERG Editions, Strasbourg, Firenze, Italy, pp 141–146
Rinntech (2009) http://www.rinntech.com/content/blogcategory/2/28/lang,english/
Ripley BD (1996) Pattern Recognition and Neural Networks, Cambridge: Cambridge University Press
Santilli M, Pelfini M (2002) Dendrogeomorphology and dating of debris flows in the Valle del Gallo, Central Alps, Italy. Dendrochronologia 20:269–284
Shroder JF Jr (1978) Dendrogeomorphological analysis of mass movement on Table Cliffs Plateau, Utah. Quaternary Research 9:168–185
Shroder J Jr, Marston RA, Stoffel M (2012) Mountain and hillslope geomorphology, treatise on geomorphology. Elsevier, Amsterdam
Schneuwly DM, Stoffel M, Dorren LKA, Berger F (2009) Three-dimensional analysis of the anatomical growth response of European conifers to mechanical disturbance. Tree Physiol 29:1247–1257
Stefanini MC (2004) Spatio-temporal analysis of a complex landslide in the Northern Apenines (Italy) by means of dendrochronology. Geomorphology 63:191–202
Stoffel M, Lièvre I, Monbaron M, Perret S (2005a) Seasonal timing of rockfall activity on a forested slope at Täschgufer (Valais, Swiss Alps)—a dendrochronological approach. Z Geomorphol 49:89–106
Stoffel M, Schneuwly D, Bollschweiler M, Lièvre I, Delaloye R, Myint M, Monbaron M (2005b) Analyzing rockfall activity (1600–2002) in a protection forest—a case study using dendrogeomorphology. Geomorphology 68:224241
Stoffel M, Bollschweiler M (2008) Tree-ring analysis in natural hazards research—an overview. Nat Hazards Earth Syst Sci 8:187–202
Stoffel M, Hitz OM (2008) Snow avalanche and rockfall impacts leave different anatomical signatures in tree rings of *Larix decidua*. Tree Physiol 28:1713–1720

Stoffel M, Conus D, Grichting MA, Lièvre I, Maître G (2008) Unraveling the patterns of late Holocene debris-flow activity on a cone in the central Swiss Alps: chronology, environment and implications for the future. Glob Planet Chang 60:222–234
Stoffel M, Bollschweiler (2009) Tree-ring reconstruction of past debris flows based on a small number of samples—possibilities and limitations. Landslides 6:225–230
Tatard L, Grasso JR, Helmstetter A (2011) Interaction between landslides, seismicity and climate in New Zealand. J Geophys Res (in press)
Therneau TM, Atkinson EJ (1997). An Introduction to Recursive Partitioning Using the rpart Routine." Technical Report 61, Section of Biostatistics, Mayo Clinic, Rochester
Thiery Y (2007) Susceptibilité du Bassin de Barcelonnette (Alpes du Sud, France) aux 'mouvements de versant': cartographie morphodynamique, analyse spatiale et modélisation probabiliste. Thèse de Doctorat, Université de Caen-Basse-Normandie, Caen, 445 pp
Thiery Y, Malet JP, Sterlacchini B, Puissant A, Maquaire O (2007) Landslide susceptibility assessment by bivariate methods at large scales: application to a complex mountainous environment. Geomorphology 92:38–59
Timell TE (1986) Compression wood in gymnosperms. Springer, Berlin
Van Asch ThWJ, Van Steijn H (1991) Temporal patterns of mass movements in the French Alps. Catena 18:515–527
van den Eeckhaut A, Muys B, Van Loy K, Poesen J, Beeckman H (2009) Evidence for repeated re-activation of old landslides under forest. Earth Surf Processes Landf 34:352–365. doi:10.1002/esp.1727
Wieczorek GF, Eaton LS, Yanosky TM, Turner EJ (2006) Hurricane-induced landslide activity on an alluvial fan along Meadow Run, Shenandoah Valley, Virginia (eastern USA). Landslides 3:95–106. doi:10.1007/s10346-005-0029-5
Williams PL, Jacoby GC, Buckley B (1992) Coincident ages of large landslides in Seattle's Lake Washington. Geological Society of America Abstract with Programs, vol 24, no. 5, p 90
Wilson RC (2005) The rise and fall of a debris-flow warning system for the San Francisco Bay region, California. In: Glade T, Anderson M, Crozier MJ (eds) Landslide hazard and risk. Wiley, Chichester, pp 493–516

J. Lopez Saez (✉) · C. Corona · F. Berger
Cemagref UR EMGR,
2 rues de la papeterie, BP 76, 38402 Saint-Martin d' Hères Cedex, France
e-mail: jerome.lopez@cemagref.fr

M. Stoffel
Laboratory of Dendrogeomorphology (dendrolab.ch), Institute of Geological Sciences, University of Bern,
Baltzerstrasse 1 +3, CH-3012 Bern, Switzerland

M. Stoffel
Climatic Change and Climate Impacts, Institute for Environmental Sciences, University of Geneva,
7, chemin de Drize, CH-1227 Carouge-Geneva, Switzerland

L. Astrade
Laboratoire EDYTEM, Bâtiment Belledonne, Campus de Technolac,
Université de Savoie–CISM,
73370 France, France

J.-P. Malet
Institut de Physique du Globe de Strasbourg, CNRS UMR 7516,
Université de Strasbourg/EOST,
5 rue René Descartes, 67084 Strasbourg Cedex, France